Preprints of the 21st IFAC World Congress (Virtual)
Berlin, Germany, July 12-17, 2020

Single Stage PLL-less Decoupled Active and Reactive Power Control for Weak Grid Interactive Inverters

Ahmad Khan, Mohsen Hosseinzadehtaher and **Mohammad B. Shadmand**

Power Electronics & Autonomous Systems Research Group
Dept. of Electrical & Computer Engineering, Kansas State University, Manhattan, KS, USA
amkhan@ksu.edu, mhosseinzadehtaher@ksu.edu, mshadmand@ksu.edu

Abstract: This paper presents a single stage phase locked loop-less (PLL-less) active and reactive power (PQ) control for single-phase weak grid interactive inverters. The absence of the PLL requirement in the proposed PQ control enhances the stability margin comparing to conventional current control approaches in both the stationary or the synchronous reference frame. Additionally, the proposed control scheme enables direct PQ control with a single loop control structure. This paper demonstrates that the proposed PLL-less PQ control scheme is asymptotically stable if the controller gains are positive. The necessary conditions for supplying the rated active power into the weak grid are derived. The provided analysis shows that certain amount of reactive power injection is necessary to avoid point of common coupling (PCC) voltage collapse when the rated active power is injected into the weak grid. Several case studies are provided to demonstrate the performance of the proposed PLL-less PQ control scheme under weak grid condition.

Keywords: PLL-less, active and reactive power control, PQ control, grid-connected inverter, weak grid

1. INTRODUCTION

Single-phase grid-connected inverter are utilized in numerous applications such as renewable energy, electric vehicle charging, HVDC transmission systems, flexible alternative current transmission systems, etc. (Khan et al., 2019; Kjaer et al., 2005). Conventionally, grid-connected inverters are controlled to mimic a current source that is injecting current into the utility grid according to the desired PQ operation set-point (Lamb & Mirafzal, 2016). In addition, grid-connected inverters also play a crucial role in supporting the utility grid (Zhang et al., 2020). For instance, grid-connection codes and standards are mandating grid interactive inverters to perform ancillary services such as power factor correction, frequency and voltage support, harmonics and unbalance compensation, power reserved control, and continuous power generation, etc. (IEEE, 2009; Khan et al., 2020; VDE, 2010).

One of the essential parts of the conventional current control for grid-connected inverters that ensures synchronization is the PLL (Blaabjerg et al., 2006; Sadeque et al., 2020; Zhong & Boroyevich, 2016). Recent literature revealed that PLL influences the small-signal stability of grid-connected inverters (Gui et al., 2019; Zhong, 2016; Zhong et al., 2016; Zhong et al., 2014). Specifically, a negative admittance increment is observed at the low range of the frequency spectrum (Farrokhabadi et al., 2019; Wen et al., 2016). According to (Wang et al., 2018), the range of this negative admittance is linked to the bandwidth of the PLL and it has been revealed that a low bandwidth PLL will guarantee control robustness. However, a low bandwidth PLL sacrifices the dynamic performance of the grid-connected inverter. Even though, with a properly designed low bandwidth PLL, enforcing the grid-connected inverter to remain stable under weak grid conditions is challenging. Hence, providing a control approach for grid-connected inverter without a PLL requirement (i.e. PLL-less) enhances the stability of an inverter interacting with a weak grid (Konstantopoulos et al., 2016).

This paper proposes a single stage decoupled PLL-less PQ control for single-phase grid-connected inverters. The proposed controller's single stage structure reduces the effort in tuning the controller's gains compared to the conventional dual loop cascaded current control methodology (Gui et al., 2017; Hosseinzadehtaher et al., 2019). The proposed control approach enables PCC current synchronization without the utilization of a PLL. Hence, avoiding instabilities that might arise due to PLL controller's non-linear nature and weak grid's large line impedance negative influence on the PCC voltage (Khan & Blaabjerg, 2018; Umar et al., 2020). Moreover, to supply the rated active power into the weak grid with the proposed PLL-less PQ control; the necessary amount of the reactive power injection is derived in this paper. This amount of the reactive power avoids PCC voltage collapse.

The remainder of the paper is organized as follows: Section 2 presents the mathematical model and derivation of the proposed single loop PLL-less PQ control for a single-phase grid-connected inverter. Then, section 3 discusses about weak grid considerations and PCC voltage collapse avoidance. Results and discussion of the paper findings are presented in section 4. Finally, section 5 concludes the paper.

2. SINGLE PHASE GRID-CONNECTED INVERTER MODELING AND CONTROLLER DESIGN

Consider the single-phase inverter that is connected to a weak grid in Fig. 1. The active power (P) and reactive power (Q) injected into the grid can be measured by utilizing the second

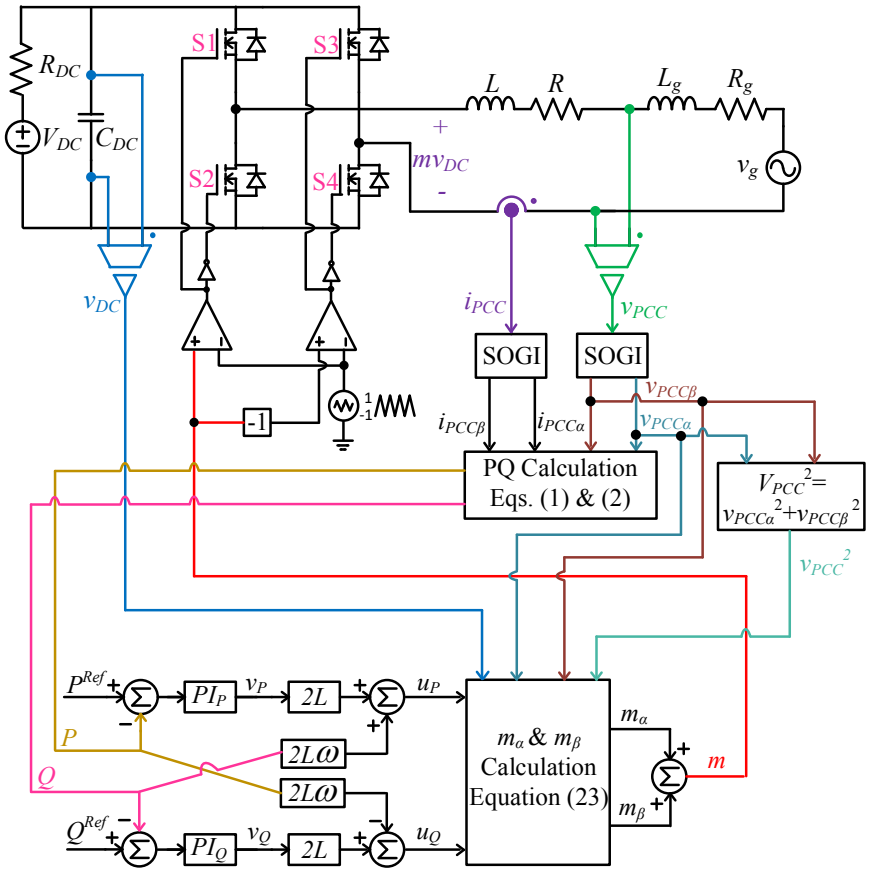

Fig. 1. Proposed single loop PLL-less PQ controller structure for single-phase grid-connected inverter

order generalized integrator (SOGI) that was developed by (Ciobotaru et al., 2006) as (1) and (2), respectively. Moreover, SOGI has unique harmonic filtering capability that makes the measurements robust to distortion imposed by weak grid conditions (Easley, Baker, et al., 2019; Easley, Hosseinzadehtaher, et al., 2019).

$$P = \tfrac{1}{2}(i_{PCC}^{\alpha} v_{PCC}^{\alpha} + i_{PCC}^{\beta} v_{PCC}^{\beta}) \tag{1}$$

$$Q = \tfrac{1}{2}(i_{PCC}^{\alpha} v_{PCC}^{\beta} - i_{PCC}^{\beta} v_{PCC}^{\alpha}) \tag{2}$$

By differentiating equations (1) and (2), the state-space model that includes active and reactive power as state variables can be determined,

$$\frac{dP}{dt} = \tfrac{1}{2}\left(\frac{di_{PCC}^{\alpha}}{dt} v_{PCC}^{\alpha} + i_{PCC}^{\alpha} \frac{dv_{PCC}^{\alpha}}{dt} + \frac{di_{PCC}^{\beta}}{dt} v_{PCC}^{\beta} + i_{PCC}^{\beta} \frac{dv_{PCC}^{\beta}}{dt}\right) \tag{3}$$

$$\frac{dQ}{dt} = \tfrac{1}{2}\left(\frac{di_{PCC}^{\alpha}}{dt} v_{PCC}^{\beta} + i_{PCC}^{\alpha} \frac{dv_{PCC}^{\beta}}{dt} - \frac{di_{PCC}^{\beta}}{dt} v_{PCC}^{\alpha} - i_{PCC}^{\beta} \frac{dv_{PCC}^{\alpha}}{dt}\right) \tag{4}$$

Furthermore, the expression for the derivatives of the stationary reference frame PCC currents i_{PCC}^{α} and i_{PCC}^{β} in (3) and (4) are deduced by applying Kirchhoff voltage law at the loop of common coupling depicted in Fig. 1. Hence, the PCC currents derivatives are as (5) and (6).

$$\frac{di_{PCC}^{\alpha}}{dt} = \frac{m_\alpha v_{DC}}{L} - \frac{v_{PCC}^{\alpha}}{L} - \frac{R i_{PCC}^{\alpha}}{L} \tag{5}$$

$$\frac{di_{PCC}^{\beta}}{dt} = \frac{m_\beta v_{DC}}{L} - \frac{v_{PCC}^{\beta}}{L} - \frac{R i_{PCC}^{\beta}}{L} \tag{6}$$

where m_α and m_β are stationary reference frame modulation indices, L is the filter inductance, and R is the filter resistance. Similarly, expression of the derivates of the stationary reference PCC voltages v_{PCC}^{α} and v_{PCC}^{β} in equations (3) and (4) are as (7) and (8).

$$\frac{dv_{PCC}^{\alpha}}{dt} = -\omega v_{PCC}^{\beta} \tag{7}$$

$$\frac{dv_{PCC}^{\beta}}{dt} = \omega v_{PCC}^{\alpha} \tag{8}$$

where ω is the angular frequency of the grid. Therefore, substituting (5), (6), (7) and (8) into (3) and (4) results in the time varying MIMO state-space system given by (9) and (10). The system is time varying because the stationary reference modulation indices m_α and m_β are multiplied by the PCC voltages. In addition, this MIMO state space control inputs are coupled in both states.

$$\frac{dP}{dt} = -\frac{R}{L} P - \omega Q + \frac{1}{2L}(m_\alpha v_{DC} v_{PCC}^{\alpha} + m_\beta v_{DC} v_{PCC}^{\beta} - v_{PCC}^2) \tag{9}$$

$$\frac{dQ}{dt} = -\frac{R}{L} Q + \omega P + \frac{1}{2L}(m_\alpha v_{DC} v_{PCC}^{\beta} - m_\beta v_{DC} v_{PCC}^{\alpha}) \tag{10}$$

where $v_{PCC} = \sqrt{v_{PCC}^{\alpha\,2} + v_{PCC}^{\beta\,2}}$. However, if the two inputs are defined as (11) and (12); the state-space in (9) and (10) transform into a simple LTI MIMO state-space as (13) and (14).

$$u_P = m_\alpha v_{DC} v_{PCC}^{\alpha} + m_\beta v_{DC} v_{PCC}^{\beta} - v_{PCC}^2 \tag{11}$$

$$u_Q = m_\alpha v_{DC} v_{PCC}^{\beta} - m_\beta v_{DC} v_{PCC}^{\alpha} \tag{12}$$

$$\frac{dP}{dt} = -\frac{R}{L} P - \omega Q + \frac{1}{2L} u_P \tag{13}$$

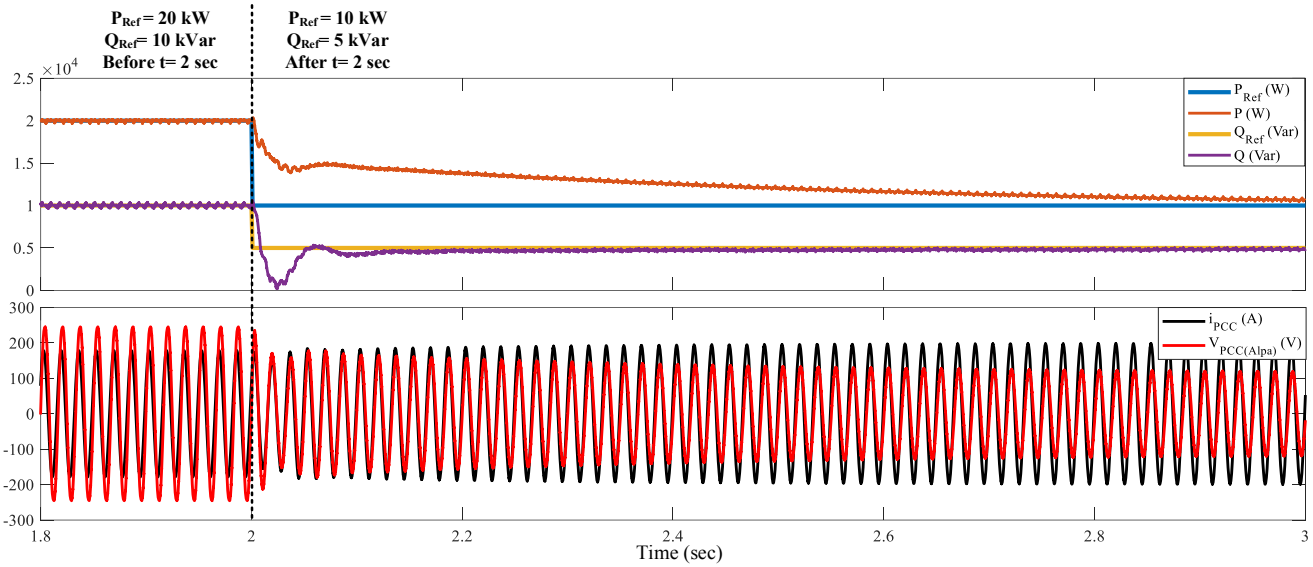

Fig. 2. Dynamic performance of the proposed single stage PLL-less decoupled PQ control

$$\frac{dQ}{dt} = -\frac{R}{L}Q + \omega P + \frac{1}{2L}u_Q \tag{14}$$

Now, consider the error on the instantaneous active and reactive power as (15) and (16),

$$e_P = P^{Ref} - P \tag{15}$$

$$e_Q = Q^{Ref} - Q \tag{16}$$

where P^{Ref} is the reference commanded active power and Q^{Ref} is the reference commanded reactive power. Moreover, the cancellation of the coupling terms in (13) and (14) is achieved by taking the following control law that includes feedback and feedforward as (17) and (18).

$$u_P = \underbrace{2L\omega Q}_{Feedforward} + \underbrace{2Lv_P}_{Feedback} \tag{17}$$

$$u_Q = \underbrace{-2L\omega P}_{Feedforward} + \underbrace{2Lv_Q}_{Feedback} \tag{18}$$

The feedback term v_P in (17) is obtained with a Proportional Integral (PI) controller as (19) that tracks the desired active power reference.

$$v_P = K_{Pp}e_P + K_{Pi}\int_0^t e_P(\tau)d\tau \tag{19}$$

Similarly, the feedback term v_Q in (18) is deduced with a PI controller as (20), this PI controller assures tracking the desired reactive power reference.

$$v_Q = K_{Qp}e_Q + K_{Qi}\int_0^t e_Q(\tau)d\tau \tag{20}$$

Moreover, substituting (19) into (17) and then place the resultant expression into (13) outcomes in the error dynamics of the active power that is shown in equation (21).

$$\frac{d^2e_P}{dt^2} = -(K_{Pp} + \frac{R}{L})\frac{de_P}{dt} - K_{Pi}e_P \tag{21}$$

Likewise, inserting (20) into (18) and then substitute the resultant into (14) outcomes in the error dynamics of the reactive power as (22).

$$\frac{d^2e_Q}{dt^2} = -(K_{Qp} + \frac{R}{L})\frac{de_Q}{dt} - K_{Qi}e_Q \tag{22}$$

The active and reactive power error dynamics in equations (21) and (22) indicate that if the controller gains K_{Pp}, K_{Pi}, K_{Qp} and K_{Qi} are positive the system is asymptotically stable. As this condition guarantees that the error dynamics eigenvalues are negative. The last step is to retrieve the original system inputs; which are the inverter stationary reference modulation indices m_α and m_β,

$$\begin{bmatrix} m_\alpha \\ m_\beta \end{bmatrix} = \underbrace{\begin{bmatrix} v_{PCC}^{\alpha} & v_{PCC}^{\beta} \\ v_{PCC}^{\beta} & -v_{PCC}^{\alpha} \end{bmatrix}}_{\mathbf{V_{PCC}}}^{-1} \begin{bmatrix} \frac{u_P + v_{PCC}^2}{v_{DC}} \\ \frac{u_Q}{v_{DC}} \end{bmatrix} \tag{23}$$

It worth mentioning that the matrix $\mathbf{V_{PCC}}$, in equation (23), singularity is an impossibility since the signals v_{PCC}^{α} and v_{PCC}^{β} are always orthogonal. Finally, the modulation index that controls the single-phase grid-connected inverter is as (24).

$$m = m_\alpha + m_\beta \tag{24}$$

The overall controller structure of the proposed PLL-less PQ control for single phase grid-connected inverters is illustrated in Fig. 1.

3. WEAK GRID CONSIDERATIONS AND PCC VOLTAGE STABILIZATION

The relation between the grid voltage and the PCC voltage with ignoring the grid parasitic resistance is given by,

$$V_{PCC} = \sqrt{V_g^2 - (\omega L_g I_{PCC})^2} \tag{25}$$

where the V_{PCC} is the magnitude of the PCC voltage, V_g is the magnitude of the grid voltage, and I_{PCC} is the PCC current magnitude. Furthermore, at unity power factor conditions the magnitude of the PCC current I_{PCC} is:

$$I_{PCC} = \frac{2P^{Ref}}{V_{PCC}} \tag{26}$$

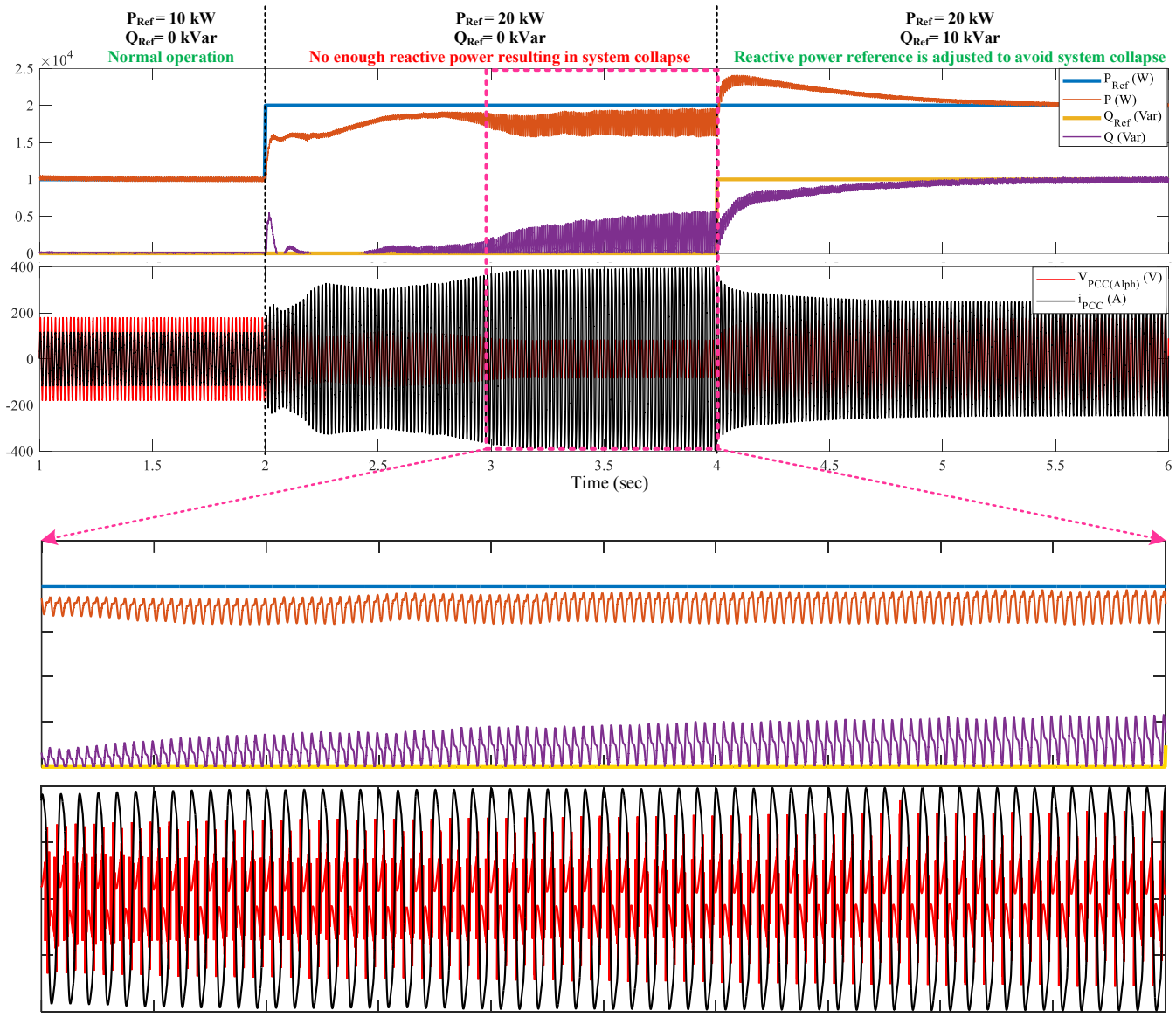

Fig. 3. Reactive power injection importance in weak grid connection

Then, by combining (25) and (26), the PCC voltage magnitude V_{PCC} is given by,

$$V_{PCC} = \sqrt{\frac{V_g^2}{2} + \sqrt{\frac{V_g^4}{4} - (2\omega L_g P^{Ref})^2}} \tag{27}$$

From (27), the grid-connected inverter maximum power injection at unity power factor is limited by,

$$\frac{V_g^4}{4} - (2\omega L_g P^{Ref})^2 \geq 0 \tag{28}$$

If the condition in (28) is not satisfied, the PCC voltage magnitude V_{PCC} becomes an imaginary value; which is not logical for a vector magnitude. In fact, such conditions mean the collapse of the PCC voltage Therefore, this imposes a limitation on supplying the rated active power into the weak grid at unity power factor. A solution for supplying the rated active power in such conditions is to supply a reactive power that compensates the voltage at the PCC. Hence, considering non-unity power factor, (27) converts into (29).

$$V_{PCC} = \sqrt{\frac{V_g^2 + 4\omega L_g Q^{Ref}}{2} + \sqrt{\frac{(V_g^2 + 4\omega L_g Q^{Ref})^2}{4} - (2\omega L_g)^2((P^{Ref})^2 + (Q^{Ref})^2)}} \tag{29}$$

Now, the condition for the maximum active power injection at non-unity power factor without PCC voltage collapse is linked to the reactive power supplied as (30).

$$\frac{(V_g^2 + 4\omega L_g Q^{Ref})^2}{4} - (2\omega L_g)^2((P^{Ref})^2 + (Q^{Ref})^2) \geq 0 \tag{30}$$

Hence, the reactive power that must be supplied to inject the rated active power is as (31).

$$Q^{Ref} \geq \frac{(2\omega L_g P^{Ref})^2 - V_g^4}{2\omega L_g V_g^2} \tag{31}$$

In other words, the rated power of the inverter can be supplied into the weak grid without a collapse of the PCC voltage.

Table I: System ratings

Parameter	Symbol	Value
Rated Power	P_{Rated}	20 kW
Switching Frequency	f_{sw}	10 kHz
Nominal Grid Frequency	ω	376.8 rad/sec
Grid Voltage Peak	V_g	$120\sqrt{2}$ V
DC-Bus Voltage	V_{DC}	420 V
DC-link Capacitor	C_{DC}	2 mF
DC source Resistance	R_{DC}	10 mΩ
Filter Inductor	L	0.5 mH
Filter Inductor Resistance	R	0.5 Ω
Grid Parasitic Inductor	L_g	1 mH
Grid Parasitic Resistor	R_g	0.1 mΩ

4. RESULTS AND DISCUISSION

The proposed PLL-less PQ control which is depicted in Fig. 1 for single phase grid-connected inverters is validated by simulation in PSIM software. The specification of the single-phase grid-connected inverter is listed in Table I. Note that, the short circuit ratio (SCR) of the grid is 1.91; which characterizes the grid as a very weak grid (Alassi et al., 2019). In more details, the SCR is defined as (32).

$$\text{SCR} = \frac{V_g^2 \Big/ \sqrt{R_g{}^2 + \omega^2 L_g{}^2}}{P_{Rated}} \tag{32}$$

The results section is divided into two subsections. The first subsection validated the developed theory and depicts the performance of the proposed PLL-less PQ control in tracking the desired active and reactive power references. Then, the second subsection validates the theory discussed regarding the reactive power injection importance to allow the inverter to inject the rated active power into the weak grid.

4.1. Dynamic Performance of the Proposed PLL-less PQ Control

The proposed PLL-less PQ control performance is depicted in Fig. 2. The system is tracking the required PQ set-points properly. As shown in Fig. 2, before instant 2 sec, the grid-connected inverter is injecting 20 kW with 10 kVar into the grid. Then, at instant 2 sec, the PQ set-point is changed to 5 kW and 5 kVar; this forces the controller to change the active and reactive power supplied into the grid. The controller settling time is less than 0.8 seconds.

4.2. Reactive Power Injection Importance with Weak Grid-Connection

A scenario has been simulated where the grid-connected inverter with the proposed PLL-less PQ control is operating initially at half of the rated active power with unity power factor operation (i.e. $P^{Ref} = 10$ kW and $Q^{Ref} = 0$ kVar). Then, suddenly the operating set-point of the inverter changes to the full rated active power at unity power factor (i.e. $P^{Ref} = 20$ kW and $Q^{Ref} = 0$ kVar). The system behaviour is depicted in Fig. 3. Moreover, it is observed that without any reactive power injection, the grid-connected inverter is gradually going to collapse when it tries to supply the rated active power (see Fig. 3 after t = 2 sec). Nevertheless, if the inverter is forced to inject a reactive power into the grid according to the inequality (31), the collapse of the system is avoided as seen in Fig. 3 after t = 4.

5. CONCLUSIONS

In conclusion, this work presented a single loop PLL-less active and reactive power control for a single-phase grid connected inverter. The proposed control closed loop error dynamics are asymptotically stable if the controller gains are positive. Also, by considering a weak grid, it was shown that for supplying the rated active power into the grid, a certain amount of reactive power is required to avoid PCC voltage collapse. Finally, the theoretical analysis was validated by simulating a 20 kW grid-connected single-phase inverter. This single-phase inverter is tied to a very weak grid with SCR of 1.91.

ACKNOWLEDGEMENT

This material is based upon work supported by the U.S. Department of Energy, Office of Energy Efficiency and Renewable Energy (EERE), Solar Energy Technologies Office, under Award Number DE-EE0008767.

REFERENCES

Alassi, A., Bañales, S., Ellabban, O., Adam, G., & MacIver, C. (2019). HVDC Transmission: Technology Review, Market Trends and Future Outlook. *Renewable and Sustainable Energy Reviews, 112*, 530-554.

Blaabjerg, F., Teodorescu, R., Liserre, M., & Timbus, A. V. (2006). Overview of Control and Grid Synchronization for Distributed Power Generation Systems. *IEEE Transactions on Industrial Electronics, 53*(5), 1398-1409.

Ciobotaru, M., Teodorescu, R., & Blaabjerg, F. (2006). *A new single-phase PLL structure based on second order generalized integrator.* Paper presented at the 2006 37th IEEE Power Electronics Specialists Conference.

Easley, M., Baker, M., Khan, A., Shadmand, M. B., & Abu-Rub, H. (2019). *Self-healing Model Predictive Controlled Cascaded Multilevel Inverter.* Paper presented at the 2019 IEEE Energy Conversion Congress and Exposition (ECCE).

Easley, M., Hosseinzadehtaher, M., Fard, A. Y., Shadmand, M. B., & Abu-Rub, H. (2019). *Computationally-efficient Hierarchical Optimal Controller for Grid-tied Cascaded Multilevel Inverters.* Paper presented at the 2019 IEEE Energy Conversion Congress and Exposition (ECCE).

Farrokhabadi, M., Canizares, C. A., Simpson-Porco, J. W., Nasr, E., Fan, L., Mendoza-Araya, P., . . . Reilly, J. T. (2019). Microgrid Stability Definitions, Analysis, and Examples. *IEEE Transactions on Power Systems*, (Early Access).

Gui, Y., Kim, C., & Chung, C. C. (2017). *Grid voltage modulated direct power control for grid connected voltage source inverters.* Paper presented at the 2017 American Control Conference (ACC).

Gui, Y., Wang, X., Blaabjerg, F., & Pan, D. (2019). Control of Grid-Connected Voltage-Source Converters: The Relationship Between Direct-Power Control and Vector-Current Control. *IEEE Industrial Electronics Magazine, 13*(2), 31-40.

Hosseinzadehtaher, M., Khan, A., Baker, M. W., & Shadmand, M. B. (2019). *Model Predictive Self-healing Control Scheme for Dual Active Bridge Converter.* Paper presented at the 2019 2nd International Conference on Smart Grid and Renewable Energy (SGRE).

IEEE. (2009). IEEE Application Guide for IEEE Std 1547(TM), IEEE Standard for Interconnecting Distributed Resources with Electric Power Systems. In (pp. 1-217).

Khan, A., & Blaabjerg, F. (2018). *Novel shunt-less filters for grid-connected transformerless photovoltaic applications.* Paper presented at the 2018 IEEE 12th International Conference on Compatibility, Power Electronics and Power Engineering (CPE-POWERENG 2018).

Khan, A., D'silva, S., Fard, A. Y., Shadmand, M. B., & Abu-Rub, H. A. (2020). On Stability of PV Clusters with Distributed Power Reserve Capability. *IEEE Transactions on Industrial Electronics*, (Early Access).

Khan, A., D'silva, S., Hosseinzadehtaher, M., Shadmand, M. B., & Abu-Rub, H. (2019). *Differential and Common Mode Active Resonance Damping Control for Shunt-less LCL Filter Based Grid-Connected PV Inverters.* Paper presented at the 2019 IEEE Power and Energy Conference at Illinois (PECI).

Kjaer, S. B., Pedersen, J. K., & Blaabjerg, F. (2005). A review of single-phase grid-connected inverters for photovoltaic modules. *IEEE Transactions on Industry Applications, 41*(5), 1292-1306.

Konstantopoulos, G. C., Zhong, Q., & Ming, W. (2016). PLL-Less Nonlinear Current-Limiting Controller for Single-Phase Grid-Tied Inverters: Design, Stability Analysis, and Operation Under Grid Faults. *IEEE Transactions on Industrial Electronics, 63*(9), 5582-5591.

Lamb, J., & Mirafzal, B. (2016). *Active and reactive power operational region for grid-tied inverters.* Paper presented at the 2016 IEEE 7th International Symposium on Power Electronics for Distributed Generation Systems (PEDG).

Sadeque, F., Benzaquen, J., Adib, A., & Mirafzal, B. (2020). Direct Phase-Angle Detection for Three-Phase Inverters in Asymmetrical Power Grids. *IEEE Journal of Emerging and Selected Topics in Power Electronics*, (Early Access).

Umar, M. F., Khan, A., & Shadmand, M. B. (2020). *A Stabilizer based Predictive Control Scheme for Smart Inverters in Weak Grid.* Paper presented at the 2020 IEEE Texas Power and Energy Conference (TPEC).

VDE. (2010). Power Generation Systems Connected to the Low-Voltage Distribution Network—Technical Minimum Requirements for the Connection to and Parallel Operation With Low-Voltage Distribution Networks. In. Germany.

Wang, X., Harnefors, L., & Blaabjerg, F. (2018). Unified Impedance Model of Grid-Connected Voltage-Source Converters. *IEEE Transactions on Power Electronics, 33*(2), 1775-1787.

Wen, B., Dong, D., Boroyevich, D., Burgos, R., Mattavelli, P., & Shen, Z. (2016). Impedance-Based Analysis of Grid-Synchronization Stability for Three-Phase Paralleled Converters. *IEEE Transactions on Power Electronics, 31*(1), 26-38.

Zhang, Z., Oluwafemi, A. W., Hosseinzadehtaher, M., & Shadmand, M. B. (2020). *Current Observer Based Predictive Decoupled Power Control Grid-Interactive Inverter.* Paper presented at the 2020 IEEE Texas Power and Energy Conference (TPEC).

Zhong, Q. (2016). Virtual Synchronous Machines: A unified interface for grid integration. *IEEE Power Electronics Magazine, 3*(4), 18-27.

Zhong, Q., & Boroyevich, D. (2016). Structural Resemblance Between Droop Controllers and Phase-Locked Loops. *IEEE Access, 4*, 5733-5741.

Zhong, Q., Ming, W., & Zeng, Y. (2016). Self-Synchronized Universal Droop Controller. *IEEE Access, 4*, 7145-7153.

Zhong, Q., Nguyen, P., Ma, Z., & Sheng, W. (2014). Self-Synchronized Synchronverters: Inverters Without a Dedicated Synchronization Unit. *IEEE Transactions on Power Electronics, 29*(2), 617-630.